RSC Advances

PAPER

View Article Online
View Journal | View Issue

Cite this: *RSC Adv.*, 2016, **6**, 107644

Electrical impedance monitoring of protein unfolding

Sandro V. de Lima,[a] Helinando P. de Oliveira[b] and Celso P. de Melo*[c]

Received 19th August 2016
Accepted 7th November 2016

DOI: 10.1039/c6ra20901g

www.rsc.org/advances

We have applied electrical impedance spectroscopy (EIS) to investigate how the dielectric characteristics of protein aqueous solutions respond to varying amounts of a co-dissolved surfactant. Using bovine serum albumin (BSA) as our model system, we followed the conformational changes of the protein molecules that result from the progressive increment in the concentration of either ionic (sodium dodecyl sulfate – SDS, and dodecyltrimethylammonium bromide – DTAB) or non-ionic (Triton X-100) surfactants, and modeled the corresponding electrical response through a modified Randles circuit. From the dielectric data, we selected the behavior of the passive layer resistance (R_{PL}) as a convenient parameter to map the conformational changes in the BSA molecules. The profile of the dielectric response of the BSA–surfactant solutions as a function of the amount of the added surfactant allows the identification of different ranges of the detergent relative concentration that can be associated to each one of the successive regimes of the surfactant–protein interaction. These results were similar to those obtained from a standard Stern–Volmer analysis of the fluorescence emission of the protein chain, with a better agreement occurring in the case of the non-ionic surfactant. We propose this novel EIS approach as a convenient alternative methodology to follow conformational changes of weakly fluorescent proteins.

Introduction

Proteins are biomolecules presenting complex function/conformation relationships that result from a delicate balance of many intermolecular/intramolecular interactions, such as hydrogen bonds, and hydrophobic and van der Waals forces. Due to these interactions, under physiological conditions proteins can self-assemble as globules, fibres and other complex shapes that are critical for the performance of their biological actions. A more complete understanding of this phenomenon continues to be of essential importance in Biology. Under certain conditions (such as variations of temperature or pH, the presence of surfactants and other dissolved molecules), the structural change involves transformation of a protein from a well-defined folded structure (its native conformation) to an unfolded state. Different conformations can then result from the folding/unfolding of the peptide chains. Therefore, a better insight on the microscopic mechanisms that control changes in protein conformation appears as an important step towards the understanding of the corresponding physiological activity.

Studies on the interactions of surfactants with globular proteins can contribute towards an improved comprehension of the action of these amphiphilic molecules, both as denaturants and as solubilizing agents for membranes of proteins and lipids.[1–6] It is also known that the presence of dissolved surfactants affects protein aggregation. Hence, a more detailed interpretation of the experimental data about the successive interactions between proteins and surfactants as a function of an increasing detergent concentration continues to be an important problem.[7] In that regard, an additional example of recent interest is the investigation of aggregation in beta amyloid proteins, a phenomenon that is believed to play a key role in the Alzheimer's disease onset: studies have shown that some gemini surfactants can promote the disassembly of amyloid fibrils.[8,9]

The interaction between surfactants and proteins can be explained through mechanisms that involve the clustering of the polar head [non-polar tail] groups of the former with the charged amino acid side chains [hydrophobic regions] of the latter. These processes are affected by the level of surfactant concentration: while isolated surfactant monomers bind to the native state as conventional ligands, micelles act as denaturants, due to the entropy dominant reactions that lead to the formation of surfactant/proteins aggregates. As we will discuss shortly, the process of protein/surfactant binding involves four successive distinct regimes.[10]

Different techniques, such as fluorescence, circular dichroism, nuclear magnetic resonance, and differential scanning calorimetry,[11–15] have been used to investigate protein/

[a]*Universidade Federal do Ceará, Crateús, Ceará, 63700-000, Brazil*
[b]*Instituto de Pesquisa em Ciência dos Materiais, Universidade Federal do Vale do São Francisco, Juazeiro, Bahia, 48902-300, Brazil*
[c]*Departamento de Física, Universidade Federal de Pernambuco, Recife, Pernambuco, 50670-901, Brazil. E-mail: celso@df.ufpe.br; Fax: +55 81 3271 0359; Tel: +55 81 2126 7612*

surfactant interactions. Fluorescence analysis, a well-established technique for protein characterization, is based on the excitation of fluorescent aromatic amino acids.[16] For instance, the bovine serum albumin (BSA) molecule has three intrinsically fluorescent amino acids, tyrosine (Tyr), tryptophan (Trp) and phenylalanine (Phe). Several studies indicate that the fluorescence emission resulting from a 295 nm excitation of a protein[17] predominantly arises from the Trp residues.[18] Phe emission has a low quantum yield (0.02, under 280 nm excitation), while the Tyr residue, which is usually present in large numbers, is a weaker emitter. Furthermore, often the corresponding emission is inhibited by the resonance transfer Tyr → Trp. We have adopted an excitation wavelength of 295 nm, which corresponds to the maximum tryptophan absorption. Of special importance to our discussion is the fact that the details of the Trp emission are highly sensitive to the nature of the immediate microscopic environment of the tryptophan residues.[18–20]

In this study, we have initially applied the fluorescence technique as a control methodology to follow the conformational changes that result from the interaction of BSA, our model protein, with surfactant molecules. By analysing the dielectric response of the corresponding aqueous solutions, we have been able to propose a new alternative method to characterize protein/surfactant interactions based on electrical impedance spectroscopy (EIS). In previous works,[21–24] we have demonstrated that EIS is a simple and convenient technique to investigate mechanisms of molecular aggregation in amphiphilic materials, such as critical micelle concentration (CMC), critical aggregation concentration (CAC), cloud point and Krafft point. In addition, we have already used the EIS technique in a preliminary exploratory investigation of the dominant molecular interactions in mixed lectin/surfactant solutions.[25]

The underlying hypothesis for the method proposed here is that in a given aqueous solution of macromolecules the prevailing charge transport and electric polarization mechanisms are dependent on the level of molecular organization at their immediate microscopic surroundings. The progressive unfolding of the polypeptide chain would promote changes in the overall conformation of the macromolecule, and, consequently, on both the percolation pathways for current transportation and on the localized regions where proper charge accumulation can occur.

Hence, our main proposal is to confirm the potential of the EIS as an alternative technique to study protein/surfactant interactions through the mapping of the electrical response associated to changes induced in the molecular organization of the macromolecules by the progressive increase in the relative concentration of the surfactant.

Experimental

Materials

The BSA protein and the surfactants used – dodecyltrimethylammonium bromide (DTAB), sodium dodecyl sulfate (SDS) and polyethylene glycol *tert*-octylphenyl ether (Triton X-100), which are representative examples of different classes of detergent molecules, were acquired from Sigma-Aldrich (USA) and used as received.

Preparation of protein/surfactants solutions

We dissolved BSA in 50 mL of deionized water and used this 0.25 g L^{-1} stock solution in all remaining experiments. Each one of the stock surfactant solutions (20 mM) of SDS, DTAB and Triton X-100 was dissolved separately in 10 mL of deionized water. Small volumes (1 mL) of the BSA solution were mixed with aliquots of the aqueous solution containing different concentration of the surfactant (*viz.* from 0 to 12 mM for SDS and DTAB, 0 to 10 mM for Triton X-100). The final concentration of BSA in the 2500 μL volume of the resulting mixture was 0.1 g L^{-1}.

Experimental techniques

We performed fluorescence measurements (emission in the 305 nm to 450 nm range, under excitation at 295 nm) using a quartz cuvette with optical length of 1 cm in a Horiba Fluorolog spectrofluorimeter. In the electrical impedance spectroscopy investigation, we used a Solartron 1260 impedance analyzer connected to a 1296 dielectric interface in the 1 Hz to 1 MHz frequency range and under a 100 mV AC voltage, with no external bias. In a preliminary analysis, we had found that the differences in the overall electrical response were negligible when an AC voltage was varied in the 5–100 mV range; hence, as a manner of preventing possible deviations when dealing with low surfactant concentrations, we choose to work in the upper voltage limit. The samples were analysed by use of a 2.5 mL Solartron 12962A sample holder.

Results

Fluorescence analysis

Since tryptophan emission accounts for most of the total fluorescence intensity of proteins, we monitored its variation to follow the changes in the conformation of the BSA molecule that resulted from the progressive increase in the concentration of different types of surfactants.

In Fig. 1a–c we show typical fluorescence emission spectra of the BSA protein when increasing amounts of the chosen surfactant (SDS, DTAB, or Triton X-100) were added to the protein aqueous solution. Upon excitation of the tryptophan residues, two main features in the BSA fluorescence emission could be identified, namely both a quenching in the BSA fluorescence intensity and a blue shift in the characteristic peaks of the protein. The emission intensity of the tryptophan residues, which exhibits a strong environmental polarity dependence,[20] is higher in hydrophobic environments than in more polar media.[26] Under physiological conditions, the less polar side chains of the Tryp residues are forced to remain in the inner hydrophobic pockets of the BSA native structure (hence maintaining minimal contact with the surrounding water molecules). However, with the increasing concentration of surfactant molecules, these residues are progressively exposed to the aqueous medium (and therefore to more polar conditions), resulting in the quenching in the BSA fluorescence intensity as

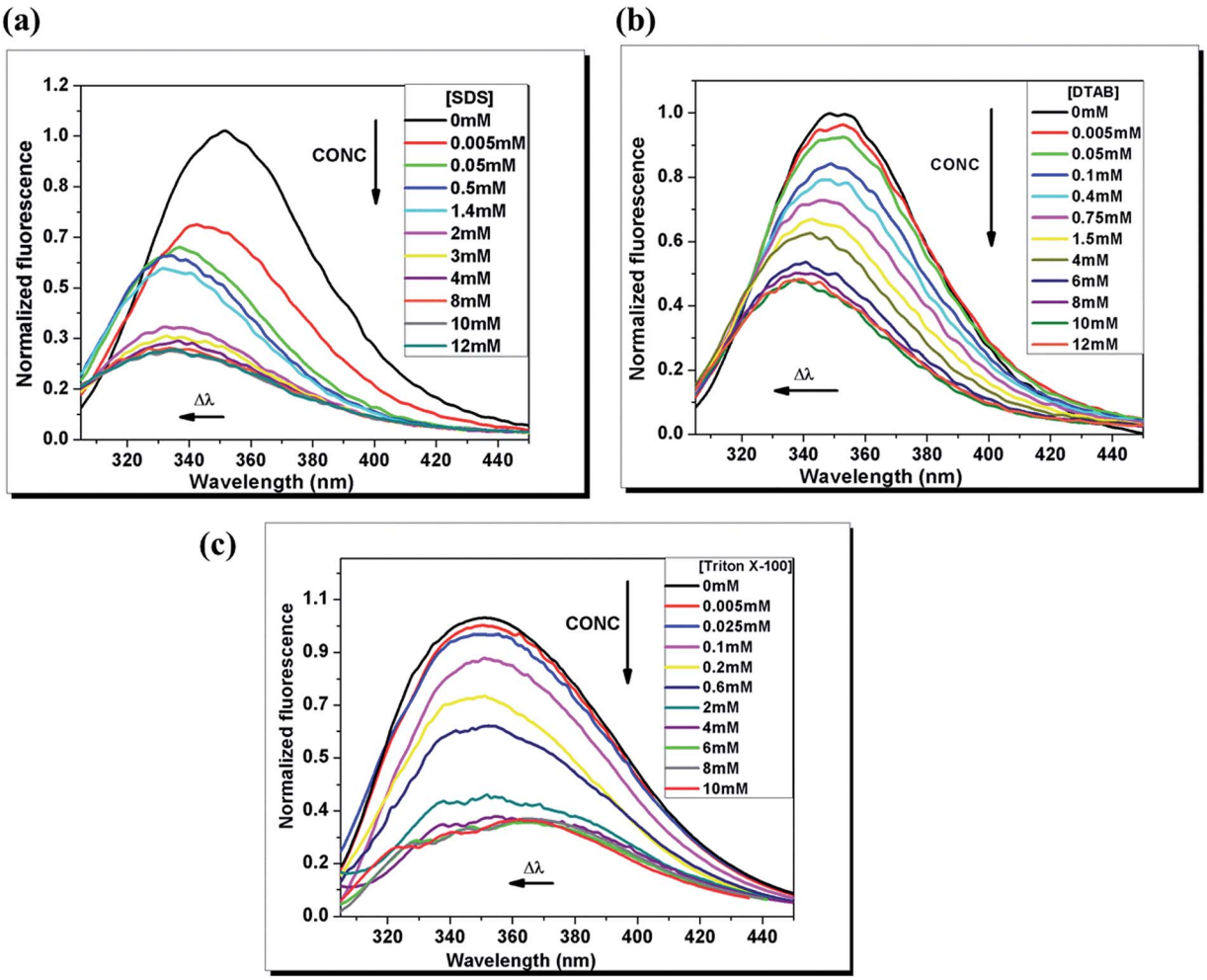

Fig. 1 Effect of the SDS (a), DTAB (b) and Triton X-100 (c) surfactants on the fluorescence spectra of BSA protein solutions.

the protein approaches a more denatured conformation. The additional band seen at 340 nm when higher TX-100 concentrations are used corresponds to the formation of dimers, as a result from the aggregation of detergent molecules.[27]

Electrical impedance spectroscopy analysis

The dielectric response of surfactant–protein aqueous solutions. In Fig. 2a–c, we show the Nyquist diagrams of BSA solutions with different concentrations of the surfactants used. Typically, two main features are evident in these diagrams: a high frequency semicircle, which is related to the bulk response of the solution, and a linear region at the low frequency regime, which is characteristic of an interfacial electrode polarization effect.[28] The latter usually arises because of the accumulation of charge carriers on interfaces, a fact that provokes a reduction in the conductivity level.

The increase in the detergent concentration causes an increment in the number of dissolved counter ions; consequently, the interfacial response is intensified and this has as a direct implication the reduction of the diameter of the characteristic Nyquist diagram's semicircle. This decrease should be more noticeable in the case of ionic surfactants, with the range of variation of the impedance being expected to be smaller when TX-100, a surfactant of non-ionic nature, is used. Even so, for all types of surfactants a noticeable change in the electric response of the solution should occur when the amount of dissolved molecules reaches the respective CMC.

Additional features in the dielectric response can be also related to the different mechanisms that are possible for the detergent/protein interaction. In fact, further increases in the surfactant concentration progressively induce the disruption of the intramolecular binding forces responsible for stabilizing the native structure of the protein, leading to its unfolding. In this condition, the polypeptide chain adopts a new 3-D molecular organization, whose mechanisms of electrical transport and charge storage differ from those prevailing in the native structure. Hence, in terms of the dielectric response of the bulk solution (*i.e.*, the surfactant/protein aqueous solution), it is reasonable to expect that a succession of characteristic changes in the electrical response of the system could be observed in the frequency domain.

Modelling the dielectric response. In search of this pattern, we looked for the most adequate circuit whose response would

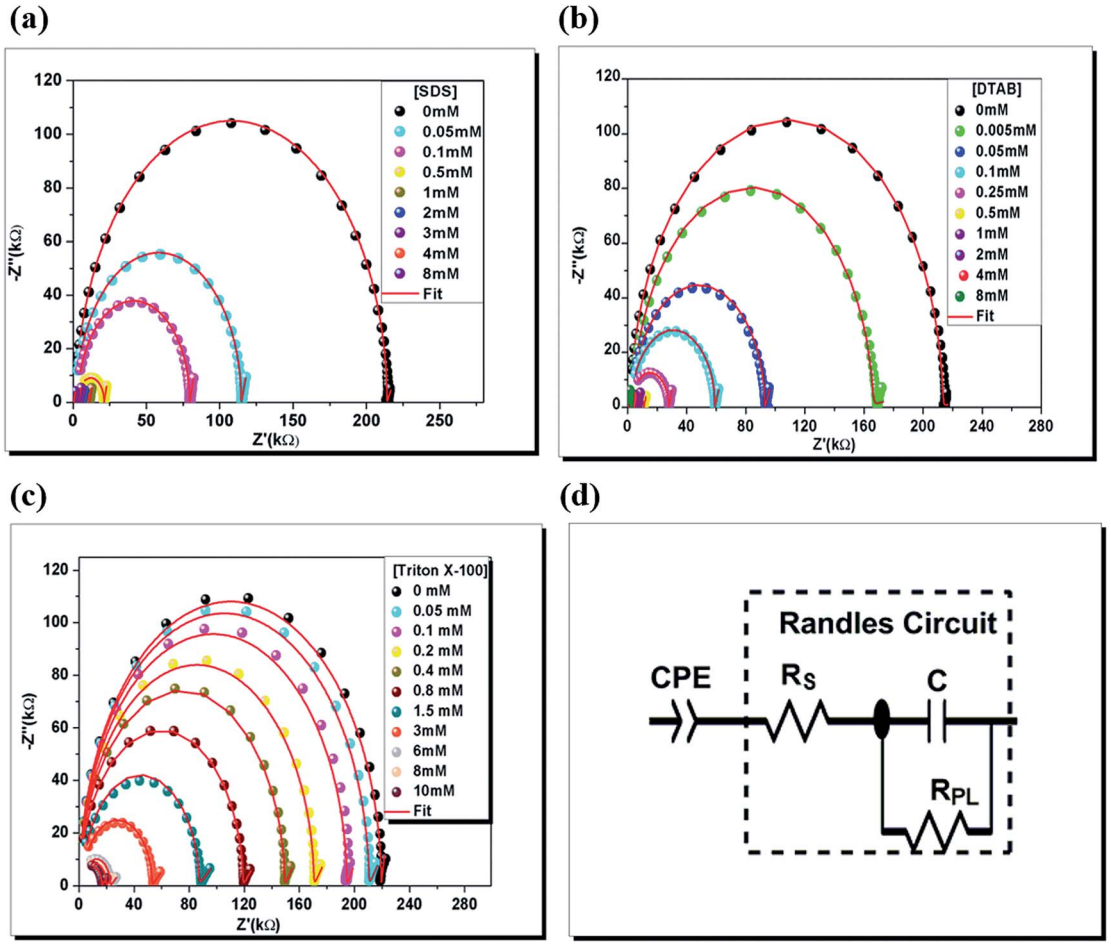

Fig. 2 Effect of the SDS (a), DTAB (b), Triton X-100 (c) surfactants on the Nyquist plots of BSA protein solution and (d) equivalent circuit used to model the dielectric response in protein/surfactant solution.

reproduce the main features of the observed dielectric response, such as relaxation (associated to the semicircle present in the diagram of Nyquist) and the progressive electrode polarization (the linear region at the low frequency limit). As before,[22,29] the Randles circuit adequately models the semicircle region of the Nyquist diagram. However, to describe correctly the linear region at low frequencies, one needs to resort to a constant phase element (CPE) $Z_{CPE} = A_0/(j\omega)^n$ associated in series with the Randles circuit.[30–36] We have then found that the electrical response of the more complex circuit shown in Fig. 2d provides the best fitting of our experimental data. While both the resistance R_S and the capacitance C characterize bulk properties of the solution, the passive layer resistance R_{PL} represents the limited charge transfer that occurs between the electrode and the bulk solution, across the double layer. An additional capacitance (CPE) has to be added in series with the Randles circuit to account for the contribution of this double layer. In fact, Moisel *et al.*[37] reported the decrease in the R_{PL} value when the concentration of BSA, which acts as an electrolyte, is increased. In addition, the unfolding process affects the adhesion of organic molecules to the metal interface, contributing to a corresponding variation of the R_{PL} value (which is strongly dependent on how extensive is the charge transfer processes across the double layer). The excellent fitting of the experimental data by the (red) continuous lines observed in Fig. 2a–c indicate that this modified equivalent electrical circuit indeed provides a good model for the dielectric response of the system. For this reason, this electric circuit was adopted as an adequate model for describing the dielectric behaviour of the protein/surfactant solution.

The real (Z') and imaginary (Z'') parts of the dielectric response of such circuit can be written as[36]

$$Z' = \frac{R_{PL}}{1+(\omega\tau)^2} + R_S + \frac{A_0}{\omega^n}\cos\left(n\frac{\pi}{2}\right) \quad (1)$$

and

$$Z'' = \frac{R_{PL}\omega\tau}{1+(\omega\tau)^2} - \frac{A_0}{\omega^n}\sin\left(n\frac{\pi}{2}\right), \quad (2)$$

where R_S represents the bulk resistance and R_{PL} the passive layer resistance, the time relaxation is $\tau = R_{PL}C$, C is the capacitance of the solution, ω is the frequency of the applied time-dependent potential, and A_0 and η are parameters of the CPE element.

Discussion

The four successive regimes of the surfactant–protein interaction

From a microscopic point of view, it is known that, as the surfactant concentration progressively increases, the amphiphilic molecules interact with the protein chains according to four successive distinct regimes:[10] specific binding, non-cooperative binding, cooperative binding and saturation (Fig. 3). In the specific binding stage, which is observed when the surfactant concentration is still very low (*i.e.*, below the corresponding CMC), charged groups of the surfactant molecules interact *via* Coulomb forces with specific charged regions of the protein.[2] With a further increase in the number of surfactant molecules in solution, the electrostatic sites in the BSA molecules will become saturated and a non-cooperative binding (which is characterized by the occurrence of hydrophobic interactions between the tail of the surfactant molecules and the less polar regions of the protein) takes place. Up to this moment, the surfactant molecules already bound to the BSA macromolecule exert negligible influence on each other. However, in the third interaction stage, the cooperative binding regime, the protein unfolding process becomes accelerated due to the collective/cooperative action of the surfactant molecules, and this leads to the complete denaturation of the BSA chains. Finally, the saturation regime is reached, where minimal interaction between proteins and additional surfactant molecules is observed, resulting in the self-assembly of the latter into micellar aggregates.

Stern–Volmer analysis of the fluorescence response

The unfolding of proteins is conventionally studied with basis on the Stern–Volmer analysis of the varying fluorimetric response of the solutions[38] (see eqn (3)). The Stern–Volmer relationship is usually adopted to describe the kinetics of the collisional processes responsible for the observed photophysical deactivation.[39] Applied to our problem, the quenching of the BSA fluorescence that follows the increase in the concentration of surfactant, [surf], obeys the relationship

$$\log\left[\frac{F_0 - F}{F}\right] = \log K_a + n \log[\text{surf}], \quad (3)$$

where $F_0[F]$ represents the fluorescence emission intensity of the protein in the absence [presence] of surfactants, K_a is the binding (or association) constant of the BSA molecule with the surfactant used, and n is a constant related to the affinity between the biomolecule and the surfactant.[6]

An important characteristic of the fluorescence technique is that, being strongly sensitive to the microscopic environment of the emitting group, it allows for a direct gathering of information about protein structures. This environmental sensitivity is a consequence of the fact that the fluorescence emission of a fluorophore can occur on the same nanosecond time scale typical of the rotational and translational motions of small molecules and protein side chains.

A novel approach to the analysis of the dielectric response

It would be reasonable to expect characteristic changes in the electrical response of surfactant–protein aqueous solutions, in a similar manner to what is observed for the fluorescence spectra. Even so, a simple inspection of the Nyquist diagrams shown in Fig. 2 is not enough to allow the identification of any noticeable changes in the regime of interaction between the BSA protein and the surfactant molecules. Hence, a detailed electrical impedance spectroscopy analysis that could identify specific changes that could occur in a relevant parameter of the electrical response of the system seems to be necessary. Ideally, the behaviour of this parameter should mimic the observed variations in the fluorescence intensity with the successive conformational changes of the macromolecules. Hence, we performed a comparative analysis of the fluorescence and electrical impedance results in search of the most adequate EIS parameter for the identification of conformational changes of proteins.

We found that the passive layer resistance R_{PL} seems to exhibit the necessary characteristics for this. In Fig. 4, we compare the variation of the maximum of fluorescence intensity

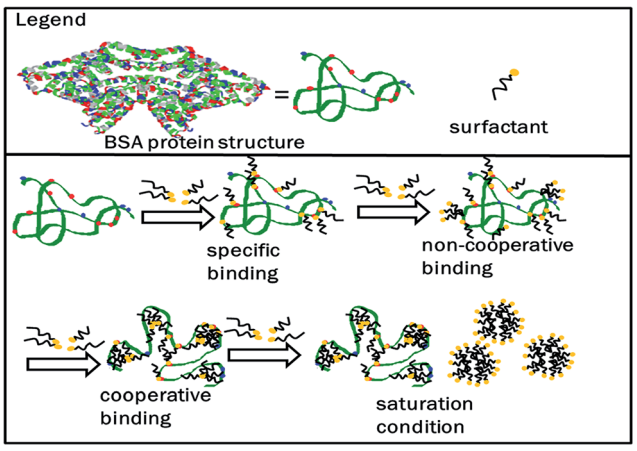

Fig. 3 Schematic representation of the BSA protein unfolding induced by surfactant molecules.

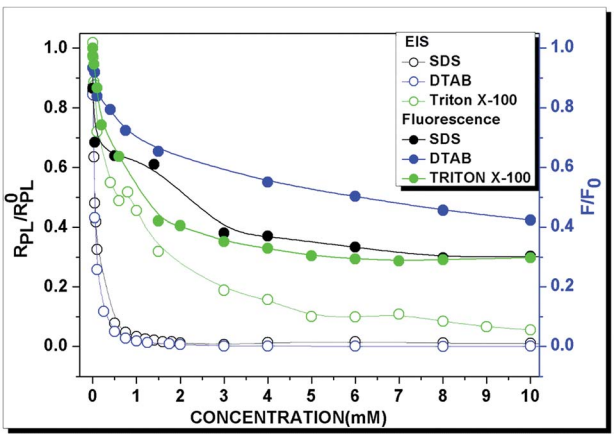

Fig. 4 Typical behaviour of the passive layer resistance and emission fluorescence intensity during of BSA unfolding induced by the progressive increase of the concentration of SDS, DTAB and Triton X-100 surfactants.

and of R_{PL}/R^0_{PL} ratio (where R^0_{PL} represents the passive layer resistance in the pristine protein solution) as the surfactant concentration [surf] increases; in fact, one can easily see that both curves exhibit the same general profile.

Based on this, we decided to examine further the question whether or not a relationship for the passive layer resistance exists that closely resembles that of the Stern–Volmer model for the fluorescence intensity. We then found that the expression

$$\log\left[\frac{R^0_{PL} - R_{PL}}{R_{PL}}\right] = \log K_1 + K_2 \log[\text{surf}], \quad (4)$$

where $R^0_{PL}[R_{PL}]$ represents the passive layer resistance of the BSA solutions in the absence [presence] of surfactants, and K_1 and K_2 are constants determined from the linear fitting of the $\log[(R^0_{PL} - R_{PL})/(R_{PL})]$ *versus* log[surf] plot, satisfies these requirements.

Comparison between the Stern–Volmer and the dielectric description of the conformational changes in the BSA molecule

To verify the accuracy of the proposed procedure, we compared the results obtained to those corresponding to a standard Stern–Volmer analysis. We examined the variation of the fluorescence emission of the tryptophan residues present in the BSA molecule (Fig. 5a–c), when the concentration of each one of the surfactants used was varied in its specific range (0.0–12.0 mM for SDS and DTAB, 0.0–10.0 mM for Triton X-100). In each one of these curves, we have identified the successive regimes of BSA–surfactant interaction, by noticing the changes in the slope coefficients of the straight line (K_2 values) fitted to each specific region. For the ionic surfactants SDS and DTAB (Fig. 5a and b), it is possible to verify that the same consecutive linear stages

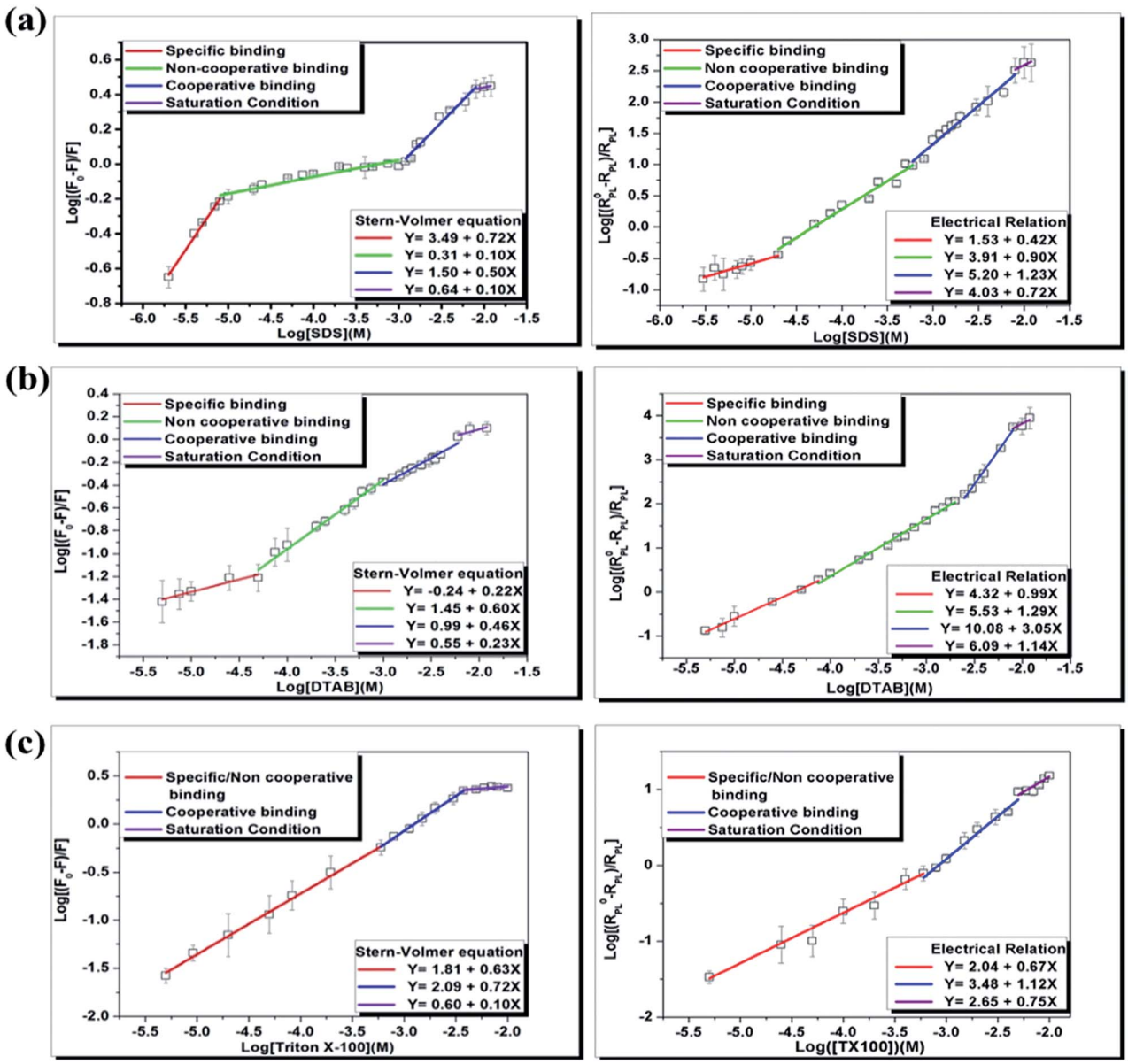

Fig. 5 Comparison between the standard fluorescence methodology and the alternative electrical impedance description of the BSA protein unfolding induced by SDS (a), DTAB (b) and Triton X-100 (c).

(binding specific, non-cooperative, cooperative and saturation condition) exist in both cases (standard and EIS method).

However, in both methods, we identified only three distinct regions of interaction when the nonionic surfactant Triton X-100 was used (Fig. 5c). The existence of three interaction regimes, instead of the four regions found in the case when ionic surfactants were used, can be associated to the nonionic nature of the Triton X-100. Since there are no charged groups in its molecular structure, the occurrence of specific interactions with the BSA macromolecule is minimized; therefore, it becomes difficult to distinguish the boundary between the specific and non-cooperative interaction regions in the curves shown in Fig. 5c. One can consider that in Fig. 5c the specific and non-cooperative regimes are described by a single straight line with a well-defined slope, in a manner that is similar to what is discussed in ref. 13.

A second important point to note is that in the Triton X-100 case the boundary between the unified specific/non-cooperative regime and the cooperative binding region appears in a rather subtle manner in the fluorescence curve (Fig. 5c). The sets of coefficients that describe the linear fitting in each one of these two regions are similar to each other, as revealed by the comparison of the slopes of the specific/non-cooperative (n = 0.63) and cooperative (n = 0.72) regimes. This could be expected, once one considers that nonionic surfactants have a lesser effect on the native structure of a protein as compared to ionic surfactants,[40] which are much stronger agents for conformation changes.[41] In addition, the level of fluorescence intensity at the last region of interaction between the BSA and the surfactant molecules (*i.e.*, the saturation condition) exhibits a weak variation. This can be taken as an indication that the unfolding of the tryptophan residues in the polypeptide chain of BSA is coming to an end, with the formation of surfactant micelles becoming the dominant process.[42]

From the electrical point view, instead, the behaviour of the passive layer resistance R_{PL} of the BSA solutions as a function of the surfactant concentration is determined by the combination of two effects. First, the progressive increase of the surfactant concentration leads to an ever-increasing conductivity of the solution (due to the continuous addition of charge carriers in the medium). In addition, changes in the slope of this variation occur due to the unfolding of the protein molecules (since that, new barriers are introduced to the conduction paths of the charge carriers). In this regard, the higher the concentration of the surfactant, more intense the second effect would become, as exemplified by the difference in the values of the angular coefficient K_2 of the dielectric response curves presented in Fig. 5c. One can explain the changes in slope in the curves of the different surfactants by taking into account the nature of the protein/surfactant interaction. Initially, the specific binding promotes only electrostatic interactions between the BSA protein and the detergent molecules dispersed in solution, which means that in this regime the variations in charge transport mainly result from the contribution of the surfactant. As the non-cooperative bindings are established, the hydrophobic interactions between the tails of the surfactant and the side chains of the protein begin to induce the unfolding of the macromolecule. As a consequence of these interactions, a molecular rearrangement that promotes changes in charge transport occurs, and this is manifested by the variation in the value of K_2. This effect is maximized in the cooperative interaction regime, as the collective action of the surfactant molecules leads to the surfactant/protein aggregation. The formation of mixed BSA/surfactant aggregates causes a new change in the charge transport, and this allows one to distinguish between the dielectric responses of the non-cooperative and cooperative regions through of the variation of the angular coefficient (see curves and respective equations in Fig. 5c). Finally, in the saturation regime, micelles and mixed BSA/surfactant aggregates begin to co-exist, and that situation corresponds to new changes in the physical chemical properties in the medium, resulting in another variation in the slope of the curves.

The characteristic concentrations that identify the different regimes, as determined by using each one of the techniques, are summarized in Table 1.

The divergence between the limiting values of the different interaction regimes as measured by the fluorescence and EIS techniques depends of the nature of the surfactant used. For instance, when ionic surfactants (such as SDS and DTAB) are added to a protein solution, both the specific/non-cooperative binding of surfactants with proteins and the level of conductivity are changed (the latter due to the dispersion of the counter ions). As a consequence, the electrical response will be affected not only by the progressive increase in the surfactant/protein interaction and in the surfactant/surfactant aggregation processes, but also by the continuous change in the baseline corresponding to the resistance of the solution. The same does not happen when the non-ionic surfactant TX-100 is used. Hence, a higher degree of agreement between the fluorescence and EIS results should be expected in this case, because the variation in the solution resistance is much smaller when counter ions are absent.

In conclusion, the impedance-based methodology here presented is able to produce results that correlate well with those obtained by use of the standard fluorescence method to investigate BSA/surfactant interactions in aqueous solutions. In special, the critical concentrations that indicate the onset of each new successive stage of the interaction are similar in both techniques, with a better agreement being observed when a non-ionic surfactant is used. It is believed that during the unfolding process the cooperative binding is marked by the

Table 1 Critical transition concentration (mM)[a]

	SB → NB		NB → CB		CB → S	
	EIS	FS	EIS	FS	EIS	FS
SDS	0.01	0.01	0.60	1.00	8.00	8.03
DTAB	0.08	0.05	2.00	1.05	8.01	6.02
Triton X-100	—	—	0.66	0.60	4.88	3.98

[a] SB – specific binding; NB – noncooperative binding; CB – cooperative binding; S – saturation. EIS: electrical impedance spectroscopy FS: fluorescence spectroscopy.

occurrence of drastic changes in the BSA conformation.[10] After comparing the effects of three different types of surfactants, one can see that this behaviour is indeed evident in the alternative procedure, and this can be verified by examining the values of slopes of the non-cooperative and cooperative regimes. The variation in the angular coefficient K_2 from 0.90 to 1.23 (SDS), 1.29 to 3.05 (DTAB) and 0.67 to 1.12 (Triton X-100) that occurs at the intersection between these two regimes is a strong evidence that the unfolding process can be adequately accompanied by EIS. These results confirm the reliability of the EIS technique when used as an alternative or complementary method for identification of the different microscopic processes that take place as an increasing number of surfactant molecules interact with protein chains.

Situations where the dielectric approach could be especially useful

We believe that the approach suggested here might be particularly useful in situations where the standard method of following the fluorescence of the amino acid residues could be not very effective. Numerous examples of proteins where the tryptophan or tyrosine residues are absent (or present in very low numbers) exist. For instance, this is the case of protamine, which does not contain these aromatic amino acids;[43] as a consequence, this protein exhibits weak intrinsic fluorescence emission, making difficult to use the standard Stern–Volmer procedure to characterize its conformational changes.[16] Another similar situation is found in the case of hemeproteins (such as hemoglobin), since the heme groups absorb radiation in the 310–360 nm range. This corresponds to the same frequency region where the tryptophan fluorescence emission occurs, and hence for that class of proteins use of the standard analysis is hindered again. Although changes in the experimental setup could fix the problem, in practical terms the study of these systems is either limited to concentration ranges below 5 μM or requires the use of fluorimeters with possibility of front-face optical configurations.[44,45]

Situations where the standard fluorescence approach fails reaffirm how important is to establish certified alternative procedures for characterizing changes in protein conformation. In this sense, the methodology of EIS presented in this study especially attractive if one considers that its implementation does not involve any direct interference with the intrinsic protein denaturing process.

Recently it came to our attention the use of EIS to evaluate the efficiency of drugs to prevent protein fibril formation,[46] where the protein was co-dissolved with a fluorescent marker (thioflavin-T). While such reporter molecules could interact with the protein of interest and modify their aggregation kinetics, the method here discussed relies entirely in the dielectric response of the target in its interaction with the aqueous medium.

Conclusions

We have introduced the idea of exploiting the electrical impedance spectroscopy technique for the investigation of the structural organization of macromolecules. For this, the variation of passive layer resistance R_{PL} of the aqueous solution of interest was determined in a manner chosen to allow the modeling of the measured impedance response through an equivalent electric circuit as a function of the concentration of the surfactant. We accomplished this in a procedure that parallels the usual Stern–Volmer fluorescence description. We have successfully used this approach to describe the conformational changes induced in a standard protein (BSA) by the presence of co-dissolved surfactants molecules. For different types of surfactants considered, both of charged (SDS and DTAB) and non-ionic (Triton X-100) nature, the impedance-based method here proposed gave reliable results in comparison to those obtained by use of the standard fluorescence approach, especially in the identification of the cooperative binding regime. Since no counter ions (which could contribute to the overall electric response of the solution) are introduced into the solution when Triton X-100 is used, we suggest that use of this non-ionic surfactant is especially advantageous for the EIS technique, which is not affected by the intrinsic fluorescence of the detergent.

Acknowledgements

The authors wish to thank the Brazilian agencies CNPq, CAPES, FINEP, FAPESB and FACEPE for their financial support. This work has been partially supported by CAPES and CNPq ELINOR Nanobiotechnology network and CNPq's INFO National Institute.

References

1 S. Deep and J. C. Ahluwalia, *Phys. Chem. Chem. Phys.*, 2001, **3**, 4583–4591.
2 C. M. C. Faustino, A. R. T. Calado and L. Garcia-Rio, *Biomacromolecules*, 2009, **10**, 2508–2514.
3 W. Gospodarczyk, K. Szutkowski and M. Kozak, *J. Phys. Chem. B*, 2014, **118**, 8652–8661.
4 D. Kelley and D. J. McClements, *Food Hydrocolloids*, 2003, **17**, 73–85.
5 S. Tardioli, A. Bonincontro, C. L. Mesa and R. Muzzalupo, *J. Colloid Interface Sci.*, 2010, **347**, 96–101.
6 T. Zhou, M. Ao, G. Xu, T. Liu and J. Zhang, *J. Colloid Interface Sci.*, 2013, **389**, 175–181.
7 S. Rocha, J. A. Loureiro, G. Brezesinski and M. d. C. Pereira, *Biochem. Biophys. Res. Commun.*, 2012, **420**, 136–140.
8 M. Cao, Y. Han, J. Wang and Y. Wang, *J. Phys. Chem. B*, 2007, **111**, 13436–13443.
9 Y. Han, C. He, M. Cao, X. Huang, Y. Wang and Z. Li, *Langmuir*, 2009, **26**, 1583–1587.
10 S. F. Santos, D. Zanette, H. Fischer and R. Itri, *J. Colloid Interface Sci.*, 2003, **262**, 400–408.
11 U. Anand, C. Jash and S. Mukherjee, *J. Phys. Chem. B*, 2010, **114**, 15839–15845.
12 U. Anand, C. Jash and S. Mukherjee, *Phys. Chem. Chem. Phys.*, 2011, **13**, 20418–20426.

13 S. De, A. Girigoswami and S. Das, *J. Colloid Interface Sci.*, 2005, **285**, 562–573.
14 S. Ghosh, S. Chakrabarty, D. Bhowmik, G. S. Kumar and N. Chattopadhyay, *J. Phys. Chem. B*, 2015, **119**, 2090–2102.
15 A. Taheri-Kafrani and A.-K. Bordbar, *J. Therm. Anal. Calorim.*, 2014, **115**, 2123–2127.
16 C. A. Royer, *Chem. Rev.*, 2006, **106**, 1769–1784.
17 V. Uversky and Y. Lyubchenko, *Bio-Nanoimaging: Protein Misfolding & Aggregation*, Elsevier Science, 2013.
18 J. R. Lakowicz and C. D. Geddes, *Topics in fluorescence spectroscopy*, Plenum Press, New York, 1991.
19 L. Marcu, P. M. W. French and D. S. Elson, *Fluorescence lifetime spectroscopy and imaging: principles and applications in biomedical diagnostics*, CRC Press/Taylor & Francis Group, Boca Raton, 2014.
20 A. B. T. Ghisaidoobe and S. J. Chung, *Int. J. Mol. Sci.*, 2014, **15**, 22518–22538.
21 E. S. Araujo, J. Rieumont, C. Nogueiras and H. P. de Oliveira, *Eur. Polym. J.*, 2010, **46**, 1854–1859.
22 S. V. de Lima and H. P. de Oliveira, *Colloids Surf., A*, 2010, **364**, 132–137.
23 H. P. de Oliveira, E. G. L. Oliveira and C. P. de Melo, *J. Colloid Interface Sci.*, 2006, **303**, 444–449.
24 S. V. de Lima and H. P. d. Oliveira, *Quim. Nova*, 2010, **33**, 1928–1932.
25 C. A. S. Andrade, H. P. de Oliveira, M. D. L. Oliveira, M. T. S. Correia, L. C. B. B. Coelho and C. P. de Melo, *Colloids Surf., B*, 2011, **88**, 100–107.
26 J. T. Vivian and P. R. Callis, *Biophys. J.*, 2001, **80**, 2093–2109.
27 F. G. Sánchez and C. C. Ruiz, *J. Lumin.*, 1993, **55**, 321–325.
28 D. S. Patil, K. Shimakawa, V. Zima and T. Wagner, *J. Appl. Phys.*, 2014, **115**, 143707.
29 S. V. de Lima, H. P. de Oliveira, C. A. S. Andrade and C. P. de Melo, *Colloids Surf., A*, 2015, **471**, 139–147.
30 B. L. Mellor, E. C. Cortés, S. Khadka and B. A. Mazzeo, *Rev. Sci. Instrum.*, 2012, **83**, 015110.
31 H. Sanabria and J. H. Miller, *Phys. Rev. E*, 2006, **74**, 051505.
32 Y. Feldman, R. Nigmatullin, E. Polygalov and J. Texter, *Phys. Rev. E*, 1998, **58**, 7561–7565.
33 F. Yu, E. Polygalov, I. Ermolina, P. Yu and B. Tsentsiper, *Meas. Sci. Technol.*, 2001, **12**, 1355.
34 I. Paul Ben, S. T. Mark, C. Andreas, L. Evgeniya and F. Yuri, *Meas. Sci. Technol.*, 2013, **24**, 102001.
35 B. L. Mellor, N. A. Kellis and B. A. Mazzeo, *Rev. Sci. Instrum.*, 2011, **82**, 046110.
36 Y. Zhao, M. Wang and J. Yao, *Procedia Eng.*, 2015, **102**, 322–328.
37 M. Moisel, M. de Mele and W. D. Muller, *Adv. Eng. Mater.*, 2008, **10**, B33–B46.
38 U. Anand, S. Ghosh, N. K. Das, N. Ghosh, R. Mondal, A. Karumbamkandathil and S. Mukherjee, *Indian J. Chem., Sect. B: Org. Chem. Incl. Med. Chem*, 2013, **52**, 1031–1040.
39 M. R. Eftink and C. A. Ghiron, *Biochemistry*, 1976, **15**, 672–680.
40 H. Durchschlag, K. J. Tiefenbach, S. Gebauer and R. Jaenicke, *J. Mol. Struct.*, 2001, **563–564**, 449–455.
41 X. Zhang, A. Poniewierski, S. Hou, K. Sozanski, A. Wisniewska, S. A. Wieczorek, T. Kalwarczyk, L. Sun and R. Holyst, *Soft Matter*, 2015, **11**, 2512–2518.
42 A. Samanta, B. K. Paul and N. Guchhait, *Biophys. Chem.*, 2011, **156**, 128–139.
43 T. Ando, M. Yamasaki and K. Suzuki, *Protamines: Isolation, Characterization, Structure and Function*, Springer, Berlin, Heidelberg, 2012.
44 S. De and A. Girigoswami, *J. Colloid Interface Sci.*, 2006, **296**, 324–331.
45 D. M. Jameson, *Introduction to Fluorescence*, CRC Press, 2014.
46 A. Affanni, A. Corazza, G. Esposito, F. Fogolari and M. Polano, *J. Phys.: Conf. Ser.*, 2013, **459**, 012049.

